

A Combined Fuzzy C-Means and Level Set Method for Automatic DCE-MRI Kidney Segmentation Using Both Population-Based and Patient-Specific Shape Statistics

Moumen T. El-Melegy

Elect. Eng. Department

Assiut University

Assiut, Egypt

moumen@aun.edu.eg

Rasha M. Abd El-Karim

Math Department

Assiut University

Assiut, Egypt

Ayman S. El-Baz

Bioengineering Department

University of Louisville

Louisville, KY, USA

Mohamed Abou El-Ghar

Radiology Department

Urology and Nephrology Center

Mansoura University

Mansoura, Egypt

Abstract—Kidney segmentation from Dynamic Contrast Enhanced Magnetic Resonance Images (DCE-MRI) is a fundamental step for the early detection of transplanted kidney function. This paper presents an accurate and automatic DCE-MRI kidney segmentation method which combines fuzzy c-means (FCM) algorithm and geometric deformable model (level set) method. In order to precisely extract the kidney from its background, the evolution of the level set contour in the proposed method is controlled by the fuzzy memberships of the pixels and both population-based and patient-specific shape model. The FCM algorithm is used to initially divide the input image into kidney and background clusters. The obtained fuzzy clustering membership is used to define the initial contour of the level set method. For segmenting the kidney of a specific patient, a number of high contrast time-point images are segmented constraining the evolution of the level set contour by the population-based shape model constructed from different subjects. As more images are segmented, the patient-specific shape model is built from the obtained segmentation results and gradually used to guide the evolution of the level set contour. The performance of the proposed method is evaluated on 40 subjects. Experimental results demonstrate the efficiency, consistency, and accuracy of the proposed method especially for low contrast images.

Keywords—kidney segmentation; DCE-MRI; fuzzy C-means; level set; patient-specific shape model.

I. INTRODUCTION

Image segmentation is a great important step in computer aided magnetic resonance imaging (MRI) image analysis, which is one of the most commonly used medical imaging techniques. The main idea of image segmentation is to partition the image into two or more regions, such that each region has homogeneous properties that are different from other neighboring regions. Accurate segmentation of kidney from Dynamic Contrast Enhanced Magnetic Resonance Images (DCE-MRI) is of great importance for the early detection of acute renal rejection. Acute rejection is the immunological response of the human immune system to the foreign kidney. It

is the most common cause of the renal failure after kidney transplantation. Given the limited number of donors, early detection of the renal rejection is essential to salvage the transplanted kidney. DCE-MRI is used to measure physiological parameters, such as transfer rates and perfusion. In order to obtain DCE-MRI, the patient is injected with Gd-DTPA contrast agent and the kidney is imaged rapidly and repeatedly. Thus, each patient has a time-series images of approximately 80 different frames that are taken for the kidney during the perfusion of the contrast agent [1], as shown in Fig.1.

Despite the advantageous of DCE-MRI imaging modality, it has several problems, such as (i) the low spatial resolution of the images because they are taken very quickly, (ii) motion made by the patient breathing, (iii) contrast changes in the images. Thus, accurate segmentation of kidney from DCE-MRI is a challenging problem.

In recent years, several dedicated research efforts have been developed to address the problem of kidney segmentation. This paper focuses on the papers that are developed for segmenting kidneys from DCE-MRI images. Abdelmunim et al. [2] presented a DCE-MRI kidney segmentation method by incorporating both image and shape prior information into a level set method. Yuksel et al. [3] introduced a framework for kidney segmentation from DCE-MRI images based on the level set method where the evolution of the level set contour is constrained by the average kidney shape prior model and the gray level density calculated using adaptive linear combinations of discrete Gaussians (LCDG) [4]. In [5], the authors proposed an automated computer-aided diagnostic (CAD) system for early diagnosis of acute renal transplant rejection. In their CAD system, the intensity information of the image and shape prior information are incorporated into the level set method to segment the whole kidney from the background.

Khalifa et al. [6, 7] developed a kidney segmentation method, in which the kidney is segmented by evolving a level set contour based on shape and visual appearance priors. The

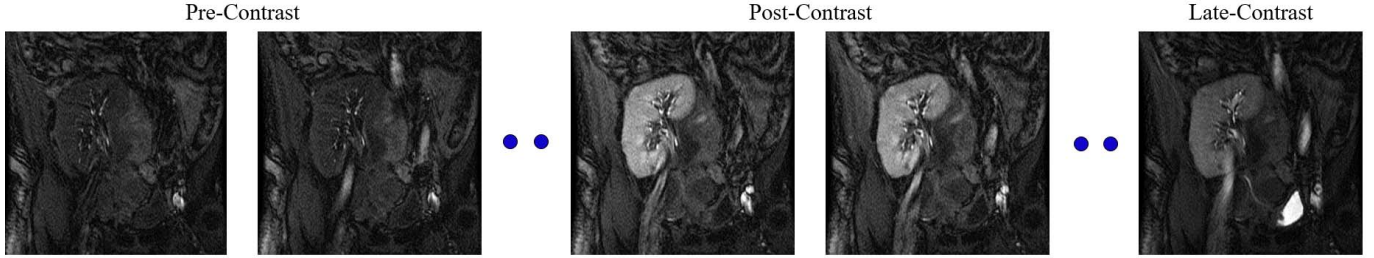


Fig. 1. An example of the DCE-MRI time sequence for one subject showing contrast agent transit.

shape prior model is constructed from a set of the manually segmented training images that are co-aligned by a rigid 2D registration to maximize their mutual information (MI) [8]. The empirical marginal gray level distributions are modeled with LCDG, and 2nd-order Markov-Gibbs random field (MGRF) is used to model the spatial interaction prior. Khalifa et al. [9] further improved their previous work in [6] by adding the 4th-order MGRF interactions to the pairwise spatial interactions that used with a weighted probabilistic kidney shape prior model and pixel-wise image intensities approximated with LCDG to constrain the evolution of the level set contour.

In order to segment the kidney from its surrounding structures, a registration step is required to handle the motion made by the patient and to align the input image to the constructed shape prior model. Unlike previous methods, Hodneland et al. [10] executed the registration step jointly with the segmentation by defining the optimization problem that is solved for both registration and segmentation simultaneously. Due to the contrast variations in the DCE-MRI images, Liu et al. [11] removed the empirical marginal gray level distributions from the speed function in [9] and constrained the evolution of the level set contour by a new 5th-order MGRF spatial interaction model and an adaptive 1st-order shape prior model.

While the previous developed kidney segmentation methods have successfully performed the segmentation of the kidney from its background, almost all of them require an accurate initialization of the level set contour that is performed manually by an expert. In order to overcome this limitation, we presented an automatic and fast DCE-MRI kidney segmentation method (FCMLS) in [12]. In FCMLS method, we used an integrated fuzzy c-means algorithm and level set method and constrained the evolution of the level set contour by kidney shape prior model and fuzzy memberships. Moreover, we used the smeared-out Heaviside function which enabled us to obtain accurate segmentation results regardless of the position of the initial level set contour.

In a similar way to our FCMLS method and to further enhance the segmentation accuracy, in this paper, we propose a novel and automated method for accurate kidney segmentation from DCE-MRI by converging ideas from fuzzy clustering [13], level set method [14], and statistical shape modeling. Due to the complexity of the kidney segmentation problem, neither the FCM algorithm nor the level set method alone can be used to

obtain fast and efficient segmentation results. Thus, it will be more efficient to integrate the FCM algorithm with the level set method to achieve fast and perfect results.

The segmentation of kidney from DCE-MRI images is a challenging problem because the gray levels of the kidney and its background are very similar which makes the boundary of the kidney hard to detect. Thus, prior information about kidney shapes is important to obtain accurate segmentation. The level set method provides the ability of incorporating the shape prior information extracted from a set of training images.

Active shape model-based segmentation is one of the most active and successful approaches in medical image segmentation that was first proposed by Cootes et al. [15]. This model employed statistical shape models trained from a set of training images that were aligned in a common coordinate system. There are two types of shape statistics, the population-based and the patient-specific shape statistics. The population-based shape is learned from a number of manually segmented training images collected from different subjects. In contrast, the patient-specific shape is trained from the segmentation results of a specific patient obtained during the segmentation process. Thus, using both population-based and patient-specific shape statistics gives more accurate segmentation results because the patient-specific shape statistics reflects the shape information of the same patient more accurately than the population-based shape statistics.

In this paper, a new and straightforward method is proposed for automatic and accurate segmentation of kidney from DCE-MRI images. The proposed method integrates the FCM algorithm with the level set method for the efficient segmentation of kidney from DCE-MRI images. We first apply the FCM algorithm on a given image to compute the fuzzy memberships of the pixels to kidney and background clusters. Then, the obtained kidney cluster is used with the shape prior information of kidney to drive the evolution of the level set contour. In order to obtain more accurate segmentation results, the proposed method uses both the population-based and patient-specific shape statistics to constrain the evolution of the level set contour. The population-based shape is constructed from a set of manually segmented kidneys of different patients. On the other hand, patient-specific shape is trained from the segmentation results of a specific patient available during the segmentation process. Unlike previous methods, using the

combined FCM algorithm and level set method in the proposed method, the convergence can be achieved after very few iterations and the computational speed is very fast whereas the accuracy of results is enhanced. Furthermore, using both the population-based and patient-specific shape statistics yields more accurate segmentation results because the patient-specific shape reflects the shape of the same patient more efficiently than the population-based shape statistics. The proposed method overcomes the accurate initialization problem of the level set contour required in previous methods, and the initial contour does not need being close to the kidney to achieve accurate segmentation results.

The rest of this paper is organized as follows. The next section introduces the main idea of the FCM clustering algorithm for image segmentation. Section III explains the geometric deformable model method. Section IV provides a detailed description of the proposed FCM level set method for kidney segmentation using both population-based and patient-specific shape models. Finally, section V presents the experimental results and quantitative evaluation, while section VI concludes the paper.

II. FUZZY C-MEANS CLUSTERING

Fuzzy c-means (FCM) is one of the most important fuzzy clustering algorithms. It is an unsupervised technique that has been widely used in medical imaging and image segmentation. The main idea behind the FCM algorithm is to distribute the data into a number of clusters where the features of each cluster are significantly different from other clusters.

For a given image $x = (x_1, x_2, \dots, x_N)$ with N pixels, the FCM algorithm classifies the pixels of the image into C clusters by iteratively minimizing the following objective function [13]:

$$J = \sum_{j=1}^N \sum_{i=1}^C \mu_{ij}^m \|x_j - v_i\|^2 \quad (1)$$

where v_i represents the centroid of the cluster i , μ_{ij} is the degree of membership of the pixel x_j in the cluster i , $\|\cdot\|$ is a norm metric, and m is a weighting exponent parameter that usually equals to 2 and determines the amount of fuzziness of the obtained segmentation results.

The membership function specifies the probability of a pixel belonging to a specific cluster where $\sum_{i=1}^C \mu_{ij} = 1$ for each pixel in the image. The membership function μ_{ij} and the centroid of the clusters v_i are updated iteratively as follows:

$$\mu_{ij} = \frac{1}{\sum_{k=1}^C \left(\frac{\|x_j - v_i\|}{\|x_j - v_k\|} \right)^{2/(m-1)}}, \quad (2)$$

$$v_i = \frac{\sum_{j=1}^N \mu_{ij}^m x_j}{\sum_{j=1}^N \mu_{ij}^m} \quad (3)$$

The membership value of a pixel depends on the Euclidean distance between the pixel and the center of its cluster. This means that the membership values of pixels to a certain cluster

will be high when they are close to the centroid of this cluster and low when they are far from the centroid. Thus, the FCM algorithm allows each pixel on the image to belong to all clusters with different degrees of membership. For a given DCE-MRI kidney image, the FCM algorithm is used to segment the image into kidney and background clusters as shown in Fig. 2.

III. GEOMETRIC DEFORMABLE MODEL

Level set method is a numerical technique that was presented by Osher and Sethian [14]. It is a powerful tool that can be used efficiently in medical image segmentation. The main idea of the level set method is to start with an initial contour which is implicitly represented using a signed distance function and evolves minimizing a defined energy function. As mentioned above, the level set method has several advantages such as the ability of handling the topological changes during curve evolution and incorporating the shape prior information of the organ to be segmented.

Let Ω and $\partial\Omega$ be the domain and a closed contour that is implicitly represented as the zero-level set of a level set function ϕ , respectively. The contour divides the domain of into interior region Ω^- and exterior region Ω^+ . The level set function is given by the signed shortest Euclidean distance from every point (x, y) in the plane to the contour. The distance is negative for the points inside the contour and positive outside, as shown in Fig. 3.

$$\begin{aligned} \phi(x, y) &> 0 & \text{if } (x, y) \in \Omega^+ \\ \phi(x, y) &< 0 & \text{if } (x, y) \in \Omega^- \\ \phi(x, y) &= 0 & \text{if } (x, y) \in \partial\Omega \end{aligned} \quad (4)$$

The area integral of a function $f(x, y)$ over the interior region $A_{Int}(\phi)$ and exterior region $A_{Ext}(\phi)$ can be defined respectively as:

$$A_{Int}(\phi) = \int_{\Omega} f(x, y) (1 - H(\phi(x, y))) dx dy \quad (5)$$

$$A_{Ext}(\phi) = \int_{\Omega} f(x, y) H(\phi(x, y)) dx dy \quad (6)$$

where $f(x, y)$ is an internal energy function of image point (x, y) that drives the front evolution and $H(\phi(x, y))$ is the Heaviside function that can be defined as follows:

$$H(\phi(x, y)) = \begin{cases} 0 & \text{if } \phi(x, y) \leq 0 \\ 1 & \text{if } \phi(x, y) > 0 \end{cases} \quad (7)$$

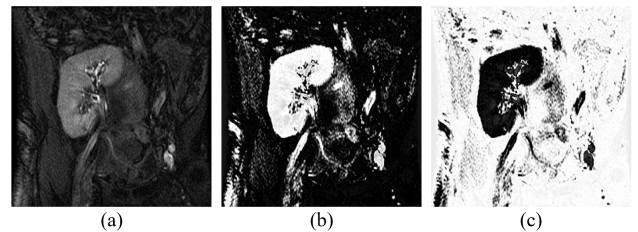


Fig. 2. The segmentation of DCE-MRI kidney image (a) into a kidney cluster (b) and background cluster (c) using the FCM algorithm.

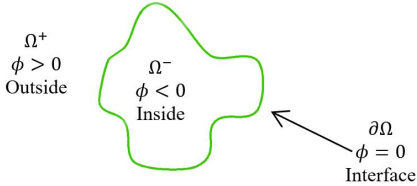


Fig. 3. Representation of the contour $\partial\Omega$ in the 2D domain Ω by a signed distance level set function.

The directional derivative of the Heaviside function H in the normal direction \vec{N} is the Dirac delta function $\delta(x, y)$ and defined as:

$$\hat{\delta}(x, y) = \nabla H(\phi(x, y)) \cdot \vec{N} \quad (8)$$

$$\nabla H(\phi(x, y)) = H'(\phi(x, y)) \nabla \phi(x, y), \quad \vec{N} = \frac{\nabla \phi(x, y)}{|\nabla \phi(x, y)|} \quad (9)$$

Thus, the line integral of a function $f(x, y)$ over the contour $\partial\Omega$ is defined using the Dirac delta function $\hat{\delta}(x, y)$ as:

$$L(\phi) = \int_{\Omega} f(x, y) \hat{\delta}(x, y) dx dy \quad (10)$$

Typically, this equation can be expressed in terms of the delta function $\delta(\phi(x, y))$ as:

$$L(\phi) = \int_{\Omega} f(x, y) \delta(\phi(x, y)) |\nabla \phi(x, y)| dx dy \quad (11)$$

$$\delta(\phi(x, y)) = H'(\phi(x, y)) \quad (12)$$

where $H'(\phi(x, y))$ is the derivative of the Heaviside function. The derivative of the Heaviside function $\delta(\phi(x, y))$ equals zero everywhere except at $\phi(x, y) = 0$. Thus, any standard sampling method will not give a good approximation to the integral in (11). In order to overcome this problem, a first order accurate smeared-out approximation of the Heaviside function and delta function will be used. The smeared-out Heaviside function is defined as:

$$H_{\varepsilon}(\phi) = \begin{cases} 0 & \phi < -\varepsilon \\ \frac{1}{2} + \frac{\phi}{2\varepsilon} + \frac{1}{2\pi} \sin\left(\frac{\pi\phi}{\varepsilon}\right) & -\varepsilon \leq \phi \leq \varepsilon \\ 1 & \varepsilon < \phi \end{cases} \quad (13)$$

where ε is a parameter that determines the size of the width of numerical smearing. Similarly, the delta function is smeared-out according to (12) as:

$$\delta_{\varepsilon}(\phi) = \begin{cases} 0 & \phi < -\varepsilon \\ \frac{1}{2\varepsilon} + \frac{1}{2\varepsilon} \cos\left(\frac{\pi\phi}{\varepsilon}\right) & -\varepsilon \leq \phi \leq \varepsilon \\ 0 & \varepsilon < \phi \end{cases} \quad (14)$$

Thus, the smeared-out Heaviside function gives a global minimizer regardless of the position of the initial contour.

IV. PROPOSED METHOD

This section describes how the FCM algorithm is combined with the level set method to efficiently segment the kidney in a

series of DCE-MRI images. As mentioned before, each patient has approximately 80 time-series images that are taken for the kidney. In contrast to the previous methods, the proposed method incorporates both the population-based and patient-specific shape prior models into the level set method to achieve more accurate segmentation.

For segmenting the kidney from a series of DCE-MRI images for a specific patient, the images are first co-aligned to a reference image that is selected among the available training images using MI affine transformation [8]. The FCM algorithm is used to initially segment all the images in the sequence into kidney and background clusters. A number of high contrast time-point images with the highest kidney cluster centroid values are segmented constraining the evolution of the level set contour by the obtained FCM clusters and population-based shape model constructed from the manually segmented images of different subjects. As more images are segmented, the patient-specific shape model is constructed from the obtained segmentation results and gradually used to guide the evolution of the level set contour. The patient-specific shape model is updated when a new segmentation result is obtained.

Consider g_t be one of the DCE-MRI serial images that is captured at time t for a specific patient. Before the current time-point image being segmented, it is co-aligned to the selected reference image using MI affine transformation. Then, it is initially segmented into kidney cluster μ_{OB} and background cluster μ_{BG} using the FCM algorithm. Using the obtained kidney cluster, the initial contour of the level set method is defined as follows:

$$\phi_0 = \mu_{OB} \geq \alpha, \quad \alpha \in (0, 1) \quad (15)$$

where α is a threshold value.

The contour of the level set method moves in the direction that minimizes an energy given by:

$$\begin{aligned} E_{seg}(\phi) = & \lambda_1 \int_{\Omega} \delta_{\varepsilon}(\phi) |\nabla \phi| dx dy + \lambda_2 \int_{\Omega} H_{\varepsilon}(\phi) dx dy \\ & + \lambda_3 \int_{\Omega} H_{\varepsilon}(\phi) f_{OB}(x, y) dx dy \\ & + \lambda_4 \int_{\Omega} (1 - H_{\varepsilon}(\phi)) f_{BG}(x, y) dx dy \end{aligned} \quad (16)$$

where λ_1 , λ_2 , λ_3 , and λ_4 are positive normalizing parameters. f_{OB} and f_{BG} are object and background functions. The first two terms in (16) control the smoothness of the level set contour and computed from the contour itself whereas the last two terms denoted as external energy attracts the contour towards the boundary of object and computed from the input image data. Thus, the design of the external energy component plays the major role in the evolutionary process. The external energy stops the evolution when the contour arrives to the kidney to keep the pixels with high kidney memberships and similar to kidney shape inside the contour while other pixels are kept outside.

The object and background functions in (16) are based on the current time-point image and defined as:

$$f_{OB}(x, y) = P_{Sh:x,y}(1) \mu_{OB:x,y} \quad (17)$$

$$f_{BG}(x, y) = P_{Sh:x,y}(0) \mu_{BG:x,y} \quad (18)$$

where $\mu_{OB:x,y}$ and $\mu_{BG:x,y} = 1 - \mu_{OB:x,y}$ denote the membership degree of the pixel (x, y) to the kidney cluster and background cluster, respectively. $P_{Sh:x,y}(1)$ and $P_{Sh:x,y}(0) = (1 - P_{Sh:x,y}(1))$ are object-background probabilities of the pixel (x, y) obtained from the shape prior model and defined as follows:

$$P_{Sh:x,y}(1) = (1 - \omega_t) PB_{Sh:x,y}(1) + \omega_t PS_{Sh:x,y}(1) \quad (19)$$

where $PB_{Sh:x,y}(1)$ and $PS_{Sh:x,y}(1)$ are the probabilities of the pixel (x, y) to be kidney obtained from the population-based (PB) and patient-specific (PS) shape prior models, respectively. ω_t is a weight factor that controls the role of population-based and patient-specific shape models in the segmentation procedure. The weight ω_t is defined as follows [16]:

$$\omega_t = \begin{cases} 0 & t \leq N_I \\ (t - N_I)/(N_b - N_I) & N_I < t \leq N_b \\ 1 & N_b < t \end{cases} \quad (20)$$

At the beginning of the segmentation process for a specific patient, the population-based shape model is only used to constrain the evolution of the level set contour ($\omega_t = 0$). After segmenting a sufficient number of time-point images N_I , the patient-specific shape model is constructed from the obtained segmentation results. The weight of the patient-specific shape model (ω_t) is gradually increased when a new time-point image is segmented. When the number of segmented time-point images exceeds N_b , the population-based shape model is no longer used and the patient-specific shape model guides the evolution of the level set contour for *future images*. The population-based and patient-specific shape models are constructed using the 1st-order shape prior method that is explained in the following section.

The Euler-Lagrange equation for the functional in (16) is given by the following gradient descent:

$$\frac{\partial \phi}{\partial t} = -\frac{\partial E_{seg}}{\partial \phi} \quad (21)$$

$$\frac{\partial \phi}{\partial t} = \delta_\varepsilon(\phi) \left(\lambda_1 \operatorname{div} \left(\frac{\nabla \phi}{|\nabla \phi|} \right) - \lambda_2 - \lambda_3 f_{OB} + \lambda_4 f_{BG} \right) \quad (22)$$

Finally, the level set function ϕ is evolving iteratively as follows:

$$\phi_{n+1}(x, y) = \phi_n(x, y) + \tau \frac{\partial \phi_n(x, y)}{\partial t} \quad (23)$$

where n is an integer instant of time $t = n\tau$ and $\tau > 0$.

A. first-order Kidney Shape Prior

Kidneys are bean-shaped organs that have a well-defined shape. Thus, it will be more efficient to incorporate the prior shape of kidney into the level set method to enhance the segmentation accuracy. As mentioned above, the contour of the level set method is constrained by both population-based and patient-specific shape prior models. The population-based shape model is constructed from a set of DCE-MRI kidney images that are collected from different subjects. The selected images are co-aligned using an affine transformation by maximizing their mutual information [8]. Then, a medical expert manually delineates the borders of the kidney to obtain the ground truth segmentation of the selected images, as shown in Fig. 4.

On the other hand, the patient-specific shape model is constructed from the segmentation results of the same patient. Thus, at the beginning of the kidney segmentation process for a specific patient, the population-based shape model is only used. As the number of segmented images of the same patient increases, the patient-specific shape model is trained and used with population-based shape model to guide the evolution of the level set contour. The population-based and patient-specific shape models are built from the segmented binary images as follows.

Let N be the total number of the selected training images and $m_i ; i = 1, \dots, N$, are associated binary images with $m_i(x, y)$ equals 1 for the kidney and 0 for the background. The probability of the pixel (x, y) to be kidney $P_{Sh:x,y}(1)$ is defined as the ratio of the counts that this pixel is classified as kidney in the selected training images to the total counts and given by:

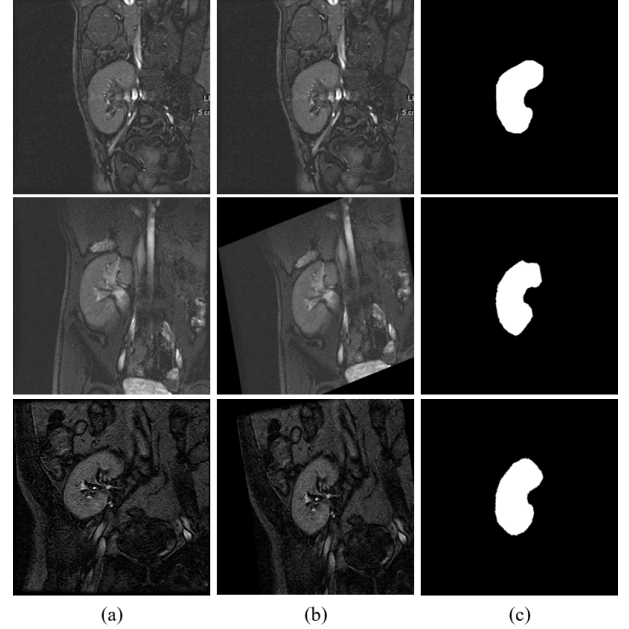


Fig. 4. Forming the population-based shape prior model from DCE-MRI training images before (a) and after MI affine transformation (b). (c) Manually segmented kidneys.

$$P_{Sh:x,y}(1) = \frac{1}{N} \sum_{i=1}^N m_i(x,y) \quad (24)$$

Thus, the probability of the pixel (x, y) to be background $P_{Sh:x,y}(0)$ is defined as follows:

$$P_{Sh:x,y}(0) = 1 - P_{Sh:x,y}(1) \quad (25)$$

The steps of the proposed FCM and level set method for automatic DCE-MRI kidney segmentation using both population-based and patient-specific shape statistics are summarized in the PBPSFL algorithm shown in Alg.1.

Alg. 1. PBPSFL Algorithm.

Input: an input DCE-MRI kidney image g .

Output: a kidney mask image.

1. Select a number of training images and select one of them as a reference image g_{ref} .
 2. Use the affine transformation to co-align the selected training images to the reference image g_{ref} .
 3. Construct the population-based shape prior model from the selected training images and their region maps.
 4. For segmenting the kidney for a specific patient do the following:
 - a. Use the FCM algorithm to initially segment all the time-point images in the sequence into kidney and background clusters.
 - b. Select a number of high contrast images N_I with the highest kidney cluster centroid values.
 - c. For each time-point image g_t ; starting with the highest contrast images.
 - Align the input image g_t to the reference image g_{ref} using MI affine transformation.
 - Initialize the contour of the level set method using the kidney cluster obtained by the FCM algorithm.
 - If $t \leq N_I$, use the population-based shape prior model and fuzzy memberships of the image to guide the evolution of the level set contour using (23).
 - If $t > N_I$, construct the patient-specific shape model from previous segmented time-point images.
 - Use both population-based and patient-specific shape models with fuzzy memberships to drive the evolution of the level set contour for segmenting the remaining time-point images.
-

V. EXPERIMENTAL RESULTS

The performance of the proposed PBPSFL kidney segmentation method has been tested on DCE-MRI data that has been collected from 40 subjects at Mansoura University Hospital, Egypt. The DCE-MRI data was acquired by bolus injecting the patient by Gd-DTPA contrast agent at a rate of 3-4 ml/s and at the dose of 0.2 ml/kgBW. The gradient-echo T1

imaging employed a 1.5 T MRI scanner with a phased-array torso surface coil. During the perfusion of the contrast agent into the organ, the kidney was imaged quickly and repeatedly. The perfusion of the contrast agent causes a contrast change in the images. Thus, each patient has approximately 80 images of size 256× 256 pixels that were obtained at 3 sec intervals before and after the perfusion of the contrast agent.

In this paper, the population-based shape model is constructed from 30 different subjects using the 1st-order kidney shape prior method, as shown in Fig. 5. In experimental results, the width of numerical smearing ε in (13) and (14) equals 3.5. The value of the threshold parameter α in (15) equals 0.1. The regularizing parameters in (16), are choosing as follows: $\lambda_1 = 4$, $\lambda_2 = 2$, $\lambda_3 = 7$, $\lambda_4 = 7$. The value of N_I and N_b in (20) equals 10 and 20, respectively.

The segmentation accuracy of the proposed PBPSFL method is quantitatively evaluated using the Dice similarity coefficient (DSC) metric [17]. The DSC metric measures the similarity between the segmentation results and ground truth of the images generated by a medical expert. The DSC metric gives values between 0 and 1, where higher DSC values indicate the better segmentation results.

To evaluate the use of patient-specific shape model with population-based shape model in enhancing the segmentation accuracy, the proposed PBPSFL method is firstly compared with FCMLS method [12]. The two methods are used to segment the kidney for all subjects. The overall segmentation accuracy for all subjects in terms of mean DSC (MDSC) and variance DSC (VDSC) values is summarized in Table I.

TABLE I. KIDNEY SEGMENTATION ACCURACY COMPARISON BETWEEN THE FCMLS METHOD AND PROPOSED PBPSFL METHOD.

	MDSC	VDSC
FCMLS	0.946	0.000634
PBPSFL	0.955	0.000192

According to the results comparison between the proposed PBPSFL method and FCMLS method in Table I, the proposed method gives more accurate segmentation results than the FCMLS method. In order to further verify the efficiency of the proposed PBPSFL method compared to FCMLS method, the

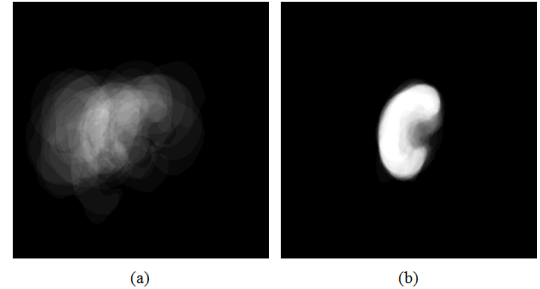


Fig. 5. The 1st-order population-based kidney shape prior model before (a) and after (b) the affine MI-based registration.

MDSC and VDSC values are computed for only the low contrast images for all subjects and the values are listed in Table II.

TABLE II. KIDNEY SEGMENTATION ACCURACY COMPARISON BETWEEN THE FCMLS METHOD AND PROPOSED PBPSFL METHOD FOR LOW CONTRAST IMAGES.

	MDSC	VDSC
FCMLS	0.897	0.00347
PBPSFL	0.941	0.00177

The comparative results in Table II show that the segmentation accuracy of the PBPSFL method has been significantly improved compared with FCMLS method for the low contrast images. Moreover, a qualitative comparison between the PBPSFL method and FCMLS method for 4 different subjects for the low contrast images is shown in Fig. 6.

From Fig. 6, it can be observed that the FCMLS method fails to detect the real boundary of the kidney for the low contrast

images, while the proposed PBPSFL method can successfully segment the kidney. It can also be observed that the proposed PBPSFL method can achieve efficient segmentation results whatever the location of the initial level set contour.

The results in Table I, Table II, and Fig. 6 show that the proposed PBPSFL method has considerable performance in segmenting kidneys in low contrast images when compared with the FCMLS method. The results also show that using patient-specific shape model with population-based shape model increases the segmentation accuracy while the method is still fast and straightforward as the FCMLS method.

To further validate the advantages of the proposed PBPSFL method, the PBPSFL method is compared with the FCMLS [12], shape-based (SB) [18], vector level set (VLS) [19], 2nd-order MGRF [6], and parametric kernel graph cut (PKGC) [20] methods. The overall mean of the segmentation accuracy for the proposed PBPSFL method and previous methods are listed in Table III.

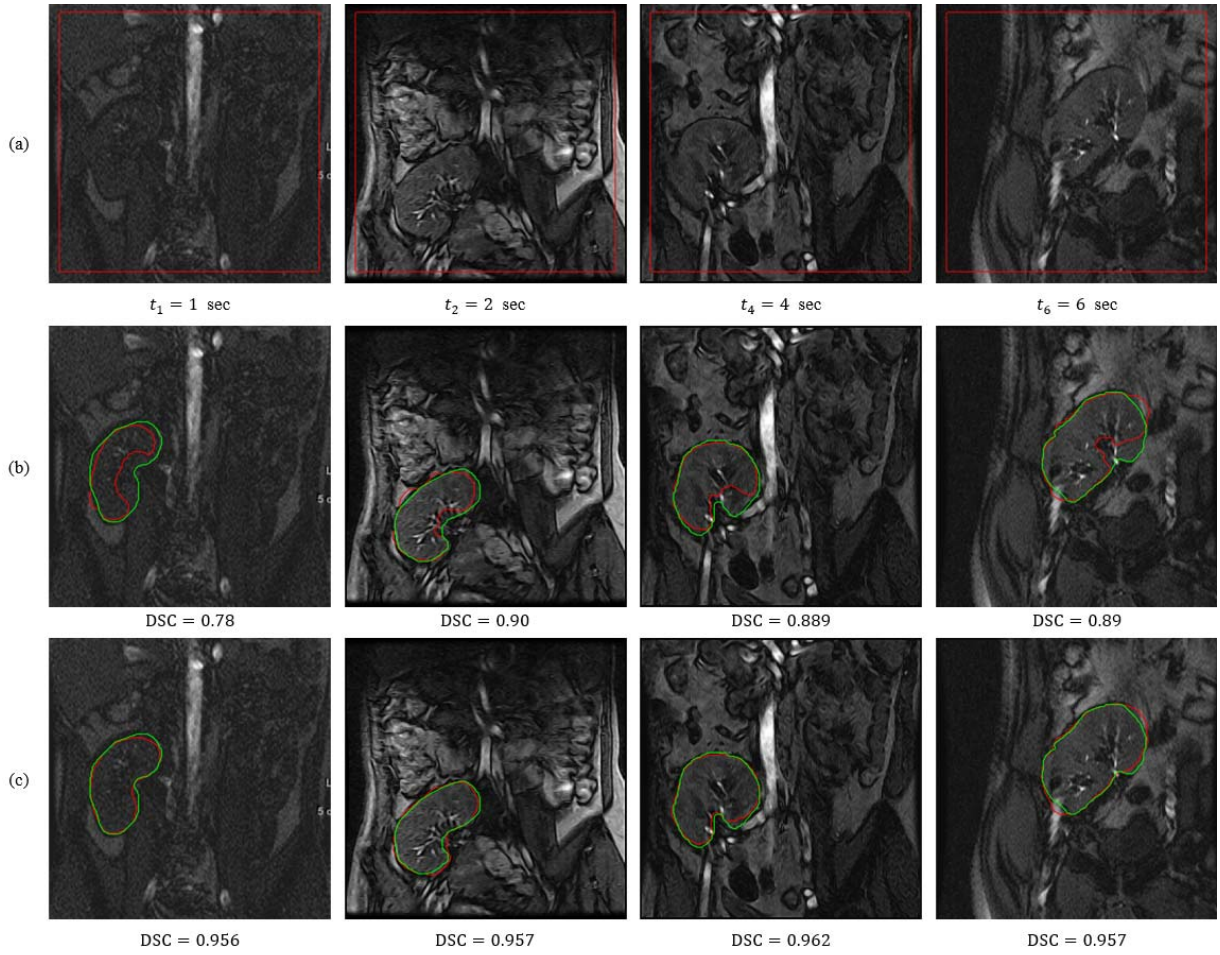


Fig. 6. (a) DCE-MRI low contrast kidney images with initial level set contour. The segmented kidneys using the FCMLS method (b) and the proposed PBPSFL method (c) shown in red and the ground truth segmentation in green.

TABLE III. KIDNEY SEGMENTATION ACCURACY COMPARISON BETWEEN THE PROPOSED PBPSFL METHOD AND PREVIOUS METHODS.

Mean DSC					
PBPSFL	FCMLS	2 nd -order MGRF	SB	VLS	PKGC
0.955	0.946	0.91	0.914	0.90	0.82

From the higher mean DSC values in Table III, the proposed PBPSFL method performs notably better compared with previous methods. Quantitative and qualitative experimental results show that the proposed method outperforms other previous kidney segmentation methods with respect to the segmentation accuracy and numbers of iterations. In the experimental results, the number of iterations of the level set method equals 60. Nevertheless, in most cases, the PBPSFL method converges after only 30 iterations.

VI. CONCLUSIONS

In this paper, a new and automatic DCE-MRI kidney segmentation method is proposed. In the proposed method, the population-based and patient-specific shape models are incorporated into the level set method to efficiently segment kidneys. The population-based shape model is constructed from a set of manually segmented kidneys of different subjects while the patient-specific shape model is built from the segmentation results for a specific subject. Moreover, the FCM algorithm is used to generate fuzzy memberships that can be used with shape models to guide the evolution of the level set contour. Using the combined FCM algorithm and level set method accelerates the convergence of the proposed method to an accurate determination of the kidney borders. Quantitative and qualitative experiments on 40 subjects show that the proposed method outperforms previous methods especially for the low contrast images. Experimental results also show that the proposed method is insensitive to the location of initial level set contour.

ACKNOWLEDGMENT

This research is supported by the Science and Technology Development Fund (STDF), Egypt (grant USC 17:253).

REFERENCES

- [1] M. Mostapha, F. Khalifa, A. Alansary, A. Soliman, G. Gimel'farb, and A. El-Baz, "Dynamic MRI-based computer aided diagnostic systems for early detection of kidney transplant rejection: A survey," in AIP Conference Proceedings (AIP), vol. 1559, no. 1, pp. 297-306, 2013.
- [2] H. Abdelmumin, A. A. Farag, W. Miller, , and M. AboelGhar, "A kidney segmentation approach from DCE-MRI using level sets," in IEEE Computer Society Conference on Computer Vision and Pattern Recognition Workshops CVPRW'08, pp. 1-6, 2008.
- [3] S. E. Yuksel, A. El-Baz, A. A. Farag, M. El-Ghar, T. Eldiasty, and M. A. Ghoneim, "A kidney segmentation framework for dynamic contrast enhanced magnetic resonance imaging," Journal of Vibration and Control, vol. 13, no. 9-10, pp. 1505-1516, 2007.
- [4] A. El-Baz and G. Gimel'farb, "EM based approximation of empirical distributions with linear combinations of discrete Gaussians," IEEE international conference in image Processing (ICIP), vol. 4, pp. 373-376, 2007.
- [5] A. El-Baz, R. Fahmi, S. Yuksel, A. Farag, W. Miller, M. El-Ghar, and T. Eldiasty, "A new CAD system for the evaluation of kidney diseases using DCE-MRI," Medical Image Computing and Computer-Assisted Intervention (MICCAI), pp. 446-453, 2006.
- [6] F. Khalifa, A. El-Baz, G. Gimel'farb, and M. A. El-Ghar, "Non-invasive image-based approach for early detection of acute renal rejection," International Conference on Medical Image Computing and Computer-Assisted Intervention, pp. 10-18, 2010.
- [7] F. Khalifa, A. El-Baz, G. Gimel'farb, R. Ouseph, and M. A. El-Ghar, "Shape-appearance guided level-set deformable model for image segmentation," 20th IEEE International Conference on Pattern Recognition (ICPR), pp. 4581-4584, 2010.
- [8] P. Viola and W. M. Wells, III, "Alignment by maximization of mutual information," International journal of computer vision, vol. 24, no. 2, pp. 137-154., 1997.
- [9] F. Khalifa, G. M. Beach, M. A. El-Ghar, T. El-Diasty, G. Gimel'farb, M. Kong, and A. El-Baz, "Dynamic contrast-enhanced MRI-based early detection of acute renal transplant rejection," IEEE transactions on medical imaging, vol. 32, no. 10, pp. 1910-1927, 2013.
- [10] E. Hodneland, E. A. Hanson, A. Lundervold, J. Modersitzki, E. Eikefjord, and A. Z. Munthe-Kaas, "Segmentation-driven image registration-application to 4D DCE-MRI recordings of the moving kidneys," IEEE Transactions on Image Processing, vol. 23, no. 5, pp. 2392-2404, 2014.
- [11] N. Liu, A. Soliman, G. Gimel'farb, and A. El-Baz, "Segmenting kidney DCE-MRI using 1st-order shape and 5th-order appearance priors," International Conference on Medical Image Computing and Computer-Assisted Intervention, Springer, pp. 77-84, 2015.
- [12] M. El-Melegy, R. A. El-karim, A. El-Baz, and M. A. El-Ghar, "Fuzzy Membership-Driven Level Set for Automatic Kidney Segmentation from DCE-MRI," IEEE International Conference on Fuzzy Systems (FUZZ-IEEE), pp. 1-8, 2018.
- [13] J. Nayak, B. Naik, and H. S. Behera, "Fuzzy C-means (FCM) clustering algorithm: a decade review from 2000 to 2014," Computational intelligence in data mining, vol. 2, pp. 133-149, 2015.
- [14] Y. Bai, X. Han, and J. L. Prince, "Geometric Deformable Models," Springer, pp. 83-104, 2015.
- [15] T. F. Cootes, C. J. Taylor, D. H. Cooper, and J. Graham, "Active shape models-their training and application," Computer vision and image understanding, vol. 61, no. 1, pp. 38-59, 1995.
- [16] Y. Shi, F. Qi, Z. Xue, L. Chen, K. Ito, H. Matsuo, and D. Shen, "Segmenting lung fields in serial chest radiographs using both population-based and patient-specific shape statistics," IEEE Transactions on medical Imaging, vol. 27, no. 4, pp. 481-494, 2008.
- [17] K. H. Zou, S. K. Warfield, A. Bharatha, C. M. Tempany, M. R. Kaus, S. J. Haker, and R. Kikinis, "Statistical validation of image segmentation quality based on a spatial overlap index," Academic radiology, vol. 11, no.2, pp. 178-189, 2004.
- [18] A. Tsai, A. Yezzi, W. Wells, C. Tempany, D. Tucker, A. Fan, and A. Willsky, "A shape-based approach to the segmentation of medical imagery using level sets," IEEE transactions on medical imaging, vol. 22, no. 2, pp. 137-154, 2003.
- [19] H. E. A. El Munim and A. A. Farag, "Curve/surface representation and evolution using vector level sets with application to the shape-based segmentation problem," IEEE Transactions on Pattern Analysis and Machine Intelligence, vol. 29, no. 6, pp. 945-958, 2007.
- [20] M. B. Salah, A. Mitiche, and I. B. Ayed, "Multiregion image segmentation by parametric kernel graph cuts," IEEE Transactions on Image Processing, vol. 20, no. 2, pp. 545-557, 2011.